heritage

MDPI

Article

The Complex Architecture of the Vault System of an Early Medieval Church

Enrico Babilio [1,*] and Silvana Rapuano [2,*]

[1] Department of Structures for Engineering and Architecture (DiSt), University of Naples "Federico II", Via Forno Vecchio 36, 80134 Naples, Italy
[2] Department of Literature and Cultural Heritage (DiLBeC), University of Campania "Luigi Vanvitelli", Via Raffaele Perla 21, 81055 Santa Maria Capua Vetere, Italy
* Correspondence: enrico.babilio@unina.it (E.B.); silvana.rapuano@unicampania.it (S.R.)

Abstract: The present work focuses on the solid modeling of the church of Santa Sofia in Benevento, Italy, and is related to a multidisciplinary research project that involved methods typical to both the humanities and mathematical engineering. Starting from the history of the church and its current configuration, a twofold objective is pursued: to give a brief account of the methodology used to analyze and virtualize the main phases of Santa Sofia and to report on the problem of modeling the church vault complex. Indeed, the 3D modeling of the church presented different levels of difficulty with some parts very easy to draw and others calling for specific geometrical analysis. In particular, to reconstruct the complex system of vaults of the church, a home-made code based on remapping Coons patches was written. The resulting 3D models of the different archeological and architectural phases of Santa Sofia are an example of virtual heritage and, being a digital content, allow for immediate sharing both to the scientific community and to a general and nonexpert audience, keeping in mind that knowledge is the means used to ensure the enhancement and preservation of cultural heritage.

Keywords: Santa Sofia in Benevento; vaults; surface reconstruction; 3D modeling; laser scanner survey

Citation: Babilio, E.; Rapuano, S. The Complex Architecture of the Vault System of an Early Medieval Church. *Heritage* **2023**, *6*, 5779–5804. https://doi.org/10.3390/heritage6080304

Academic Editor: Devrim Akca

Received: 7 June 2023
Revised: 28 July 2023
Accepted: 6 August 2023
Published: 9 August 2023

1. Introduction

The use of virtual models is widespread in many fields, from architecture to mechanical and aeronautical engineering to documentation, enhancement and protection of cultural heritage.

Virtual reconstructions are among the digital processes that have become standard in the cultural heritage sector of the humanities, being both a method of visualization accepted in the education and knowledge transfer fields, and a research tool [1]. Specifically, the virtual reconstruction of ruined artifacts of relevant importance is a very active research field, which calls for approaches allowing a rigorous line of thinking from surveys of survived parts to models [2]. In the case of artifacts of interest in archeology, quite often, the lost parts exceed what is preserved. Therefore, the information collected through a survey in the field may largely be insufficient [3].

When other data sources are available, the lack of information in the field survey may not be a critical limitation to the investigation, since in archeology, it is customary to collect and compare information from very different sources, such as written documents, iconographic and epigraphical remains, and so on. The matching of a hypothesis with artifacts from other similar and coeval contexts also becomes helpful. In particular, when the artifact comes from remote ages and has a complex history, it is mandatory that the virtual reconstruction be based on numerous verified data and conducted with reliable tools.

Solid modeling of architectural artifacts that are relevant as cultural heritage, and also in terms of archeological importance, requires that knowledge and skills from different

scientific and professional backgrounds be brought together. This procedure applies regardless of whether the modeling and related final products are aimed at the general public or a small group of experts.

This paper is related to a multidisciplinary research project that involved typical methods from very different fields such as medieval archeology, history, archival science, mechanics and computer graphics. The research, which began in January 2020, aimed at the solid modeling of the main archeological and architectural phases of the church of Santa Sofia (Figure 1a,b), located in the historical center of Benevento (N 41°7′47.14″ E 14°46′57.436″), a small town in Southern Italy, situated about 200 km south of Rome and 60 km east of Naples.

a **b**

Figure 1. The church of Santa Sofia in Benevento: the Baroque façade (**a**); rear view (**b**).

The reconstruction initiative arose from the need to deepen the results of a multiyear research [4–7], which had already identified several historical–archeological phases, and developed as a twofold study.

Firstly, starting from the survey of the church and the virtual reconstruction of its current configuration, other main layouts assumed over time have been the objects of solid modeling, in order to verify the archeological hypotheses [8]. Indeed, the church, dating back to the Lombard domination, is one of the most important examples of early medieval architecture and has undergone many restorations over time.

Secondly, but not less important in terms of possible practical implications, the study aimed at the development of textured 3D models and a multimedia product to enhance the site [9]. Indeed, the ease of transmission and communication of digital content inherently allows for its replicability and ensures its dissemination to a nonexpert audience and to the scientific community is more immediate [10].

Similarly, the present paper has a twofold objective: to give a brief account of the methodology used to analyze and virtualize the major phases of Santa Sofia and to report on the specific problem of modeling the church vault complex.

Indeed, the surveying and virtual reconstruction of vaults and domes is an active field, and among the many noteworthy studies, we mention a few.

A complete model of the vault of the entrance hall of Villa Reale of Monza, Italy, chosen as an example to test and integrate different kinds of survey methodologies (manual, topographic, photogrammetric and laser scanner), was presented in [11]. A laser survey of a special ribbed umbrella dome decorated with interlaced arches and surmounting the entrance tower of Villa Rufolo in Ravello, near Salerno, Italy, was described in [12]. In [13], a structure from motion (SfM) technique, which is the process of estimating the 3D structure of an object or, in general, a scene from a set of 2D images, as photographs, was

tested to study the geometry of the vault system of the Gothic church of Saint Gervais and Saint Protais in Paris, France. In [14], the recognition of specific suitable approximating shapes was exploited to deploy and map to the plane a vault in Palazzo Roncioni in Pisa, Italy, entirely covered by an 18th-century fresco, which could be generated by combining portions of different cylindrical surfaces. In [15], focusing on the case of the Magio Grasselli palace in Cremona, Italy, a method to analyze the cloister vaults of two main rooms was introduced. The two vaults, which are almost coeval, seem to be characterized by similar construction systems. However, the obtained HBIM (Historic Building Information Model [16]) allowed the detection of differences due to the brick assembling and their texturing techniques. In [17], a process aimed at determining the nondegenerate real quadric surface that best fits the point cloud of simple or compound vaults was provided, also demonstrating the complementarity between descriptive geometry and algorithm-based approaches. A parametric model, also usable for documentation and structural analysis, was developed to model ribbed vaults in [18]. A NURBS-based approach (NonUniform Rational B-Spline [19]) was used in [20] to model the majority of the Basilica of San Marco in Venice, Italy, including domes with profiles modeled through lofting or a network of curves. In [21], a methodology of geometric decomposition into hierarchically organized elements and digital reconstruction was applied to study the vaulting system of the atrium of Palazzo Mazzonis in Turin, Italy, also reporting two alternative rules of composition: one involving the geometric intersection of the main surface with secondary shapes, such as cylinders, cones, portions of torus, spheres, ellipsoids or ovaloids; the other involving the cutting of portions of the main surface typically with pairs of vertical planes and filling the resulting interval with surfaces generated by sections resting on the edges of the cut main surface. In [22], the analysis on the Mausoleum of Galla Placidia in Ravenna, Italy, allowed the recognition that its apparently irregular pseudo-dome, set on a parallelogram, cannot be obtained by the revolution of a curve. In [23], a strategy to define 3D parametric models for ribbed vaults was proposed and tested on the two Gothic churches of San Lorenzo and Santa Maria di Donnaregina in Naples, Italy, starting from the shape grammar approach. For the purpose of virtual reconstruction, the global geometry of the network of ribs and webbing of the stellar vault and cross-vault system of the Inner City Parish Church in Budapest, Hungary, was analyzed in [24] and in [25], respectively, using a laser scanner point cloud.

In the case we deal with in this paper, the vault surface reconstruction from the point cloud was complicated by the fact that none of the 22 vaults covering the ambulacra of the church of Santa Sofia (see Section 2.2 for details) can be approximated with basic geometric shapes. Therefore, functions approximating the vault surfaces were carefully selected and tailored. Note that by choosing control parameters appropriately, these functions include the quadric surfaces used in [17] as special cases. In addition, by virtue of proper remapping, they can be used to approximate vaults characterized by general platform, while research in the area of virtual vault reconstruction deals with the case of square, rectangular or trapezoidal vaults [23]. For the scope of this work a home-made code was developed in the *Mathematica* environment [26].

The paper is organized as follows: A concise overview of the history and the current configuration of the church is reported in Section 2, where the rendered models, actually a part of the results of this study, are also shown in advance, for the sake of the clarity of descriptions. The materials and methods used in developing the work are described in Section 3. The specific problem of modeling the church vault complex, delving into the mathematical problem underlying the reconstruction of surfaces from a discrete set of points, is treated in some depth in Section 4, where the process is also detailed in terms of a pseudo-code. The results of the reconstruction of the system of vaults is reported in Section 5. Finally, Section 6 closes the paper with some remarks.

2. Brief Details about the Church

2.1. Historical Overview

It is generally believed that the foundation of the church, now known for its distinctive star-shaped plan, dates back to 758 AD at the behest of Arechis II, Duke of Benevento, from that year until 787. It was dedicated to the Divine Wisdom of Christ (Ἁγία Σοφία in ancient Greek, from which the Italian name of Santa Sofia comes), similarly to the preexisting and renowned church of Constantinople. In 774, or a little earlier, Arechis II aggregated a Benedictine women's monastery there, which was placed under the dependencies of Montecassino, and entrusted its management to his sister (whose name may have been Gariperga) [6].

The church underwent several renovations that changed its appearance. One of the first interventions occurred around 1038 when Abbot Gregorio junior had the Romanesque bell tower built [27,28]. Later, there was the construction of the cloister and other works ordered by Abbot Giovanni IV, in the 12th century [29], and the portal with the lunette (depicting Christ Enthroned, the Virgin on the right and San Mercurio Martyr on the left with a kneeling figure at his side, possibly Giovanni IV himself, Figure 2), probably in the 13th century, and still present and perfectly preserved in the façade (Figure 1a).

Figure 2. The lunette surmounting the entrance gate.

The building, severely damaged by the earthquake of 5 June 1688, which caused the collapse of the Romanesque bell tower, underwent restoration at the behest of the Archbishop of Benevento, Vincenzo Maria Orsini, the future Pope Benedict XIII. The original star-shaped plan, transformed according to Baroque style, was made circular and a new rectangular central chapel replaced the original main apse. In addition, a new masonry fence was built to surround the space in front of the entrance (Figure 3a). Reconsecrated in February 1701 and damaged again by the earthquake of 14 March 1702, the building underwent new restoration work, entrusted to Carlo Buratti. A new bell tower was built in 1703 at a distance of 26 m to prevent its eventual collapse from causing damage as had happened in 1688. The church was reopened for worship by 1708.

Affected by an intervention in the 19th century (Figure 3b), with the demolition of the masonry fence and the construction of two side chapels, the church was the object, between 1951 and 1957, of the restoration conducted by Antonino Rusconi: based on available documents and archeological traces found, Rusconi restored the main apse and the original star-shaped plan, but saved the Baroque façade (Figure 3c,d) [7,30,31].

Because of its historical importance, the church has been a part of the UNESCO World Heritage list since 2011, in the serial site "The Lombards in Italy, the places of power (568–774 AD)".

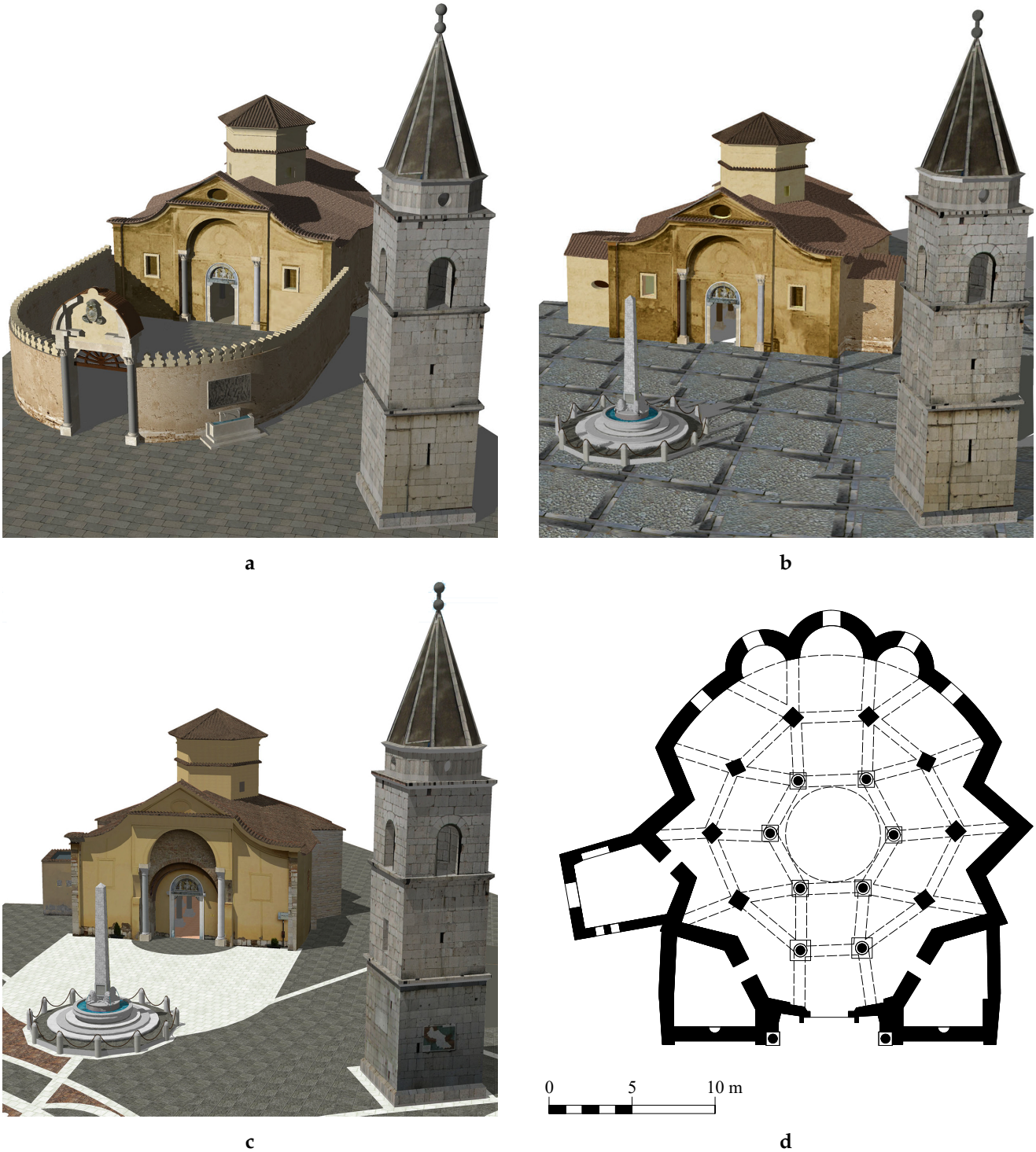

Figure 3. Three configurations of the church: the reconstruction dating back to the early 18th century, after 1688 and 1702 earthquakes, with the masonry fence on behest of Orsini and the bell tower rebuilt in 1703 (**a**); the new configuration after an intervention realized in the 19th century, with the demolition of the masonry fence and the addition of two side chapels (**b**); the current configuration after Rusconi's mid-20th-century restoration and some other minor interventions at the turn of the last quarter of the 20th century and the first decade of the 21st century, the last of which was aimed at inclusion on the UNESCO World Heritage List. Note the white area in front of the church that, with its limestone pavement, recasts the courtyard included in the 18th-century fence (**c**); the current church floor plan (**d**).

Such a serial site collects fortresses, churches and monasteries distributed throughout the Italian peninsula, such as the Tempietto Longobardo in Cividale del Friuli (Udine), the monastic complex of San Salvatore and Santa Giulia in Brescia, the castrum of Castelseprio-Torba (Varese), the Tempietto del Clitunno in Campello (Perugia), the Basilica of San Salvatore in Spoleto and the Sanctuary of San Michele in Monte Sant'Angelo (Foggia) [32].

2.2. The Architecture of the Church in Its Current Configuration

The church has a peculiar architectural layout [4,33], with a central plan, a vaulted ceiling and the ambit wall that follows, for the most part, a star-shaped profile (Figure 3d), with influences and reminiscences of early Christian and Byzantine art. To the north, where the presbytery area was located, there are three contiguous apses [4,29] that open into the perimeter wall, which has a circular development there. Beyond the presbyterial area, the ambit wall takes a star-shaped profile.

The interior space (see Figure 4) is characterized by circular columns and pillars with square cross-sections forming a central hexagon and a surrounding decagon, both having the same center. The six columns of the hexagon and two columns of the decagon are formed by perusal elements: shafts, capitals of the classical age and, as bases, inverted ancient capitals. The eight pillars are surmounted by early medieval pulvinos.

Figure 4. The interior of the church with the entrance behind the point of view. The six columns supporting the tiburium, some vaults of the two ambulacra and the three apses with remains of early medieval frescoes visible on the apsidal basins [34] can be seen.

There are two ambulacra, with the inner one between the hexagon and the decagon and the outer one placed between the decagon and the ambit wall.

On the pillars, columns and the ambit wall are placed arches made of reused bricks and flat tiles, bounding 22 vaults of various shapes covering the two ambulacra. The vault complex, especially in the outer ambulacrum, has been altered at least twice in history, namely in Orsini's 18th-century intervention and Rusconi's 20th-century restoration. However, the shapes and positions of the vaults of the inner ambulacrum, which are probably more intact, and the system of all the arches suggest that the current exterior vaults are also consistent with the original ones.

In the center is a dome with a tiburium. This is not the original one, as it is taller and was built, along with the façade, in the Baroque period, at the behest of Archbishop

Orsini, as mentioned above. Finally, the perimeter wall, made by reusing ancient materials arranged in *opus mixtum* (Latin for "mixed work"), was obtained with alternating rows of tuff blocks and brick [4,5].

3. Materials and Methods

Reconstructing the archeological phases of a historic building is a complex task, especially for those cases where the use of the structure has been constant over the centuries. When such a condition occurs, the documentary material to take into account is usually copious and varied in typology, and the research workflow includes several steps, some conducted at the same time, and some at other times, and can be summarized as:

i. The search and analysis of sources, usually divided into
   (a) archeological,
   (b) archival,
   (c) bibliographic,
   (d) epigraphical,
   (e) photographic;
ii. The formulation of a reconstruction hypothesis on the lost parts;
iii. The survey of the current layout or of the existing parts;
iv. The reconstruction of the various phases in a backward fashion from the current layout to the earliest one.

3.1. Archeological Evidences

As recalled above, the church has been modified several times, each time losing parts of the original stratigraphy.

No excavation has ever been conducted in the church except for the one by Rusconi in the 1950s, which was carried out according to the rules that were customary at that time. Therefore the stratigraphic approach of recording all the emerged evidences as required by the scientific method commonly accepted nowadays was unfortunately not applied. A few documents remain of Rusconi's activities, such as some technical drawings and photographs attesting to some of the findings made with the removal of the floor (including that of the foundation of the star-shaped perimeter, or the *opus sectile* pieces of the original flooring, and so on) and the reroofing and removal from the walls of the stucco and plaster layer from the Baroque period [35], and a paper [36] where the author himself shows a plan of the church with reconstructive hypotheses and clarifies his interpretation of the structure, with some archeological explanations.

Hence, more recent archeological studies have been based on the direct observation of the church elevations by also comparing traces of building or restoration work with information obtained from historical and iconographic documentation.

With regard to the first phase, from the 8th to the 9th century, the original technique of brick and tuff rows was graphically surveyed, studied and compared with other similar masonry of early medieval structures in Benevento. It was possible to distinguish the original masonry, which had been spared and incorporated into the 18th-century masonry and then brought to light in Rusconi's restoration, because it was placed in an undercut. All the spolia of the church were also analyzed, studied and catalogued [4].

Excavations conducted in 2000–2001 by the Archeological Superintendency of Benevento in the square in front of the church during the resurfacing revealed a complex stratigraphy and intercepted some elements related to the original layout of the church. The documentation of the excavation, however, remained unpublished for a long time and lacked the analyses and in-depth studies necessary to understand and reconstruct the stratigraphy. Currently, the team of medieval archeologists from the Department of Literature and Cultural Heritage (DiLBeC), at the University of Campania "Luigi Vanvitelli", is proceeding with a systematic study of the materials and structures, thanks to the authorization granted by the Superintendency to Marcello Rotili.

It has been recognized that, at a short distance from the entrance to the church, there are traces of curvilinear walls and some rounded elements made of mortar and stone conglomerates, with their height spanning from 60 cm to 120 cm. The rounded elements can be interpreted as the foundations of columns. In addition, their distribution and the traces of curvilinear walls are consistent with the plan of a forceps narthex, similar to those found in buildings of late antique or Byzantine architecture, such as San Giovanni in Laterano, the mausoleum of Santa Costanza, both in Rome (Italy), and the basilica of San Vitale in Ravenna (Italy) [7]. Another new finding from the excavations concerns the foundation of the church on an earlier burial nucleus dating back to the 5th up to 7th century.

The above-mentioned portal with lunette (Figure 2) in the façade, probably dating back to the 13th century, is the only relevant archeological remain of the long-lasting second phase, from the 11th to the 15th century.

In terms of archeological findings, with regard to the third phase (18th up to 19th century), which started with Orsini's restoration, the cuts in the masonry of the central apse (which are still visible outside the church, Figure 1b) are consistent with and confirm the demolition of the circular wall of the apse itself, which was then replaced by a rectangular chapel. Finds made by the Superintendency during excavations in 2000–2001 also revealed the exact location of the foundation of the masonry fence.

3.2. Archival, Bibliographic, Epigraphical and Photographic Sources

In the analysis and virtual reconstructions of the more recent phases (Figure 3b,c), it was possible to rely not only upon archival and bibliographic sources, but also on a vast repertoire of iconographic materials: surveys (plans, sections and elevations by Rusconi [36] and Ferrante [37], who also drew sketches); photographs (such as those taken inside and outside the church by Luigi Intorcia [38]); drawings (the interior of the church was portrayed by Achille Vianelli in 1871 [39]; exterior views of the church were made by Carlo Labruzzi in 1789, by Carl Wilhelm Weisbrod in 1806 [40], and by an unknown 19th-century painter [41]); and city maps of Benevento (as Casselli Map dating back to the year 1781 [40]).

Indeed, thanks to photographs, previous plans and sections recorded before the 1950s' intervention, it was possible to accurately reconstruct the interior and floor plan of the church at the time of its circular layout. The cited drawings allowed the appearance of the masonry fence to be discovered, as well as its crowning battlements, the monumental gate and the fountain decorated with a Roman sarcophagus front, as shown in Figure 3a. The plan of the masonry fence was taken from Casselli's map, which shows the entire development of the wall, and confirmed by the small piece shown in the Superintendency's technical drawings related to the aforementioned 2000–2001 excavation.

Moreover, the information from epigraphs is very important, such as those that report news about the reconstruction of the bell tower (such as that inside of the bell tower itself whose translation from Latin is: "While here he was rebuilding the bell tower—erected in another place by the Benedictine Abbot Gregorio, as the surviving epigraph informs—by the violence of the earthquake on 5 June 1688 destroyed from the foundations, he had almost completed it when he was—having been damaged by another earthquake on 14 March 1702—forced to level it to the ground, finally raised it to the top Friar Vincenzo Maria of the order of preachers Cardinal Orsini, archbishop of Benevento, protector of the canons regular of the congregation of the Most Holy Savior and perpetual commendatory of Santa Sofia in the year 1703") or the construction of the current fountain (the epigraph walled at the base of the obelisk above the fountain basin, dedicated to Charles-Maurice de Talleyrand-Périgord, prince of Benevento from 1806 to 1814, where it reads: "In honor of the excellent Prince Charles-Maurice for serving the public good, by the citizens of Benevento, in the year 1809"); see Figure 3b,c.

For the second phase, an epigraph embedded in the current bell tower presents an important chronological reference to date the construction of the first bell tower. Its

translation is: "Supported by the spirit of Christ, Gregorio the younger raised on a new foundation this valuable pyramid; being prince the illustrious Pandolfo with his son, the illustrious abbot undertook this turreted building." This information regarding the presence of a bell tower was used in the 3D reconstruction to collocate the solid near the church, following an indication also found in historical texts [28,37].

For the earliest phase, relating to the foundation of the church, much historical information and the first iconographic representation of the building, a miniature depicting Duke Arechis II presiding over the construction of the church, come from the collection of documents, entitled *Chronicon Sanctae Sophiae* [42]. From the miniature, which is very schematic and symbolic, it is possible to learn that a pictorial apparatus covered the entire interior of the church, and it confirms the presence of the tiburium and a probable narthex in front of the church. Finally, closing the circle, important data on that narthex and the early layout of Santa Sofia come from the study of the documentation and materials related to the 2000–2001 excavations, as already mentioned in Section 3.1.

3.3. Digital Survey

A laser scanner survey was carried out between the end of January and the beginning of February 2020, using the survey facilities (Leica BLK360 Laser Scanner and Cyclone Register 360 [43]) of the ReD (Ricerca e Didattica. Italian for: Research and Teaching) laboratory of DilBeC, Vanvitelli University. To survey the church, from both inside and outside, the 3D sensor was located in several positions. We henceforth call such positions as setups, the total number of setups in the survey project as the setup count and the set of data points from a single setup as a setup cloud. To avoid or minimize shaded parts, the distribution of setups (Figure 5a) was designed in advance.

The first setup was approximately set in the center of the hexagon of the tiburium, the next six in the inner ambulacrum and ten in the outer ambulacrum, in a similar spiral, connecting two consecutive setups with an ideal straight arrow ($1 \rightarrow 2 \rightarrow 3 \cdots$). Other setups (from 18 to 20) were collocated inside the three rooms around the outer ambulacrum. Once the interior of the church was completed, to survey the façade, the side walls and the exterior of the apses, the laser scanner was placed at 11 locations outside the church, thus leading to the additional acquisition of data on the fountain, square and bell tower (as well as some useless data on other surrounding buildings). For the sake of completeness, upon the assembly of the cloud with data from the 31 setups, the existence of what appeared to be a wall of a thickness that was not compatible with the others was discovered, and on subsequent verification, it was found to be a small service room, separated from the sacristy (setup 18) by means of a thin wooden partition wall. For such a reason, the very last setup (BLK360_3503964_Setup32 in Figure 5a, using the label automatically assigned by the scanner), leading to the setup count totaling 32 (Figure 5b), was not in line with our choice to fully survey the interior of the church first.

To limit the size of the raw data that needed to be stored, the acquisition was performed with the *point density mode* set to *fast*, leading to a resolution of 20 mm at 10 m and an approximate scan size of 3 million points [44]. By means of Cyclone Register 360, a cloud-to-cloud alignment based on shared geometry between scans [45] was performed and 90 links, i.e., connections between two different setup locations, were automatically detected. Hence, a bundle cloud of about 3.8×10^7 points (Figure 6) was obtained.

Note that the total point count was largely less than the sum of the points in the 32 setup clouds because of the cloud-to-cloud overlap, which is the percentage of overlapping points between couples of setups (37 % average, 4 % min, 63 % max). The symmetric matrix graphically shown in Figure 5b reports the overlapping between setups, with data taken from the report of Cyclone Register 360, then postprocessed in *Mathematica*, to express the percentage of overlapping according to a suitable color scaling. Notably, the large overlap between setups 1 through 17 was somehow expected because of the spiral path used when placing the scanner inside the church.

Finally, an overall bundle error for all links in the bundle of 0.01 m and a strength, which is the relative stiffness of the constraints on the link with respect to different directions, of 69 % were reported.

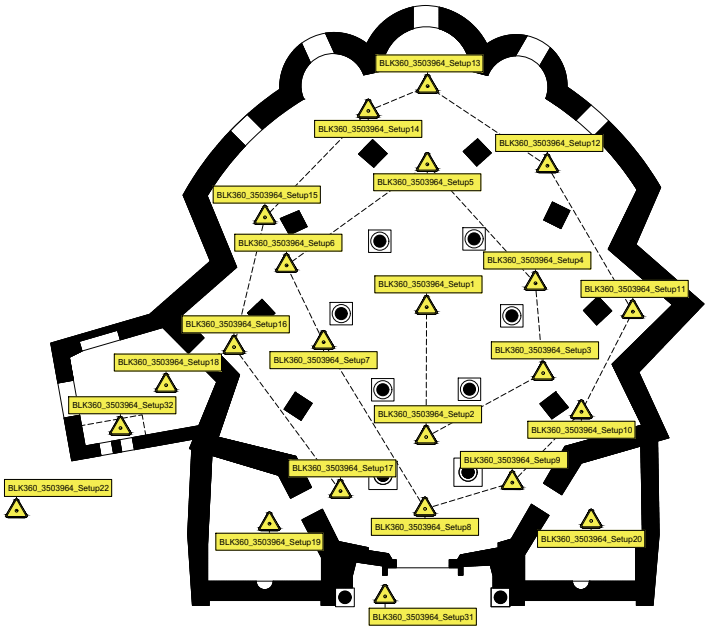

a

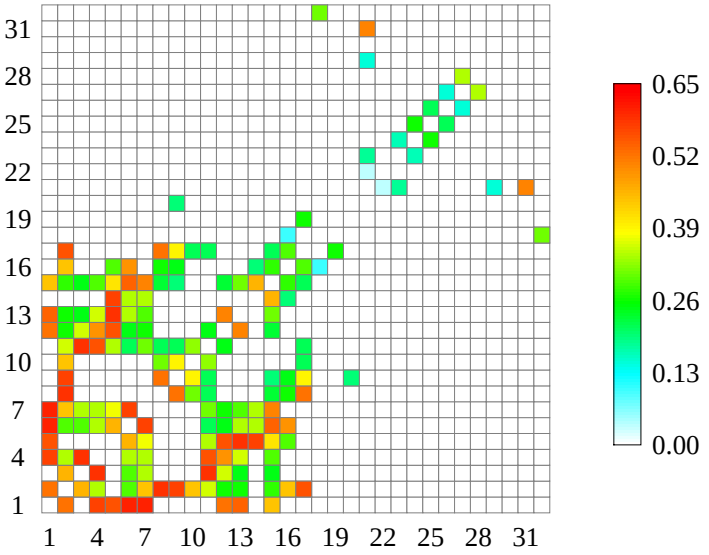

b

Figure 5. The distribution of some of the setups (**a**), which shows the positions within the point cloud that correspond to the actual locations of the sensor while scanning, and a visualization of the overlap matrix (**b**), which is a symmetric matrix whose entries express the percentage of overlapping of two setup clouds. Due to this definition, the entries along the main diagonal represent the self-overlap of the *i*th setup cloud, actually 1 (100 %), which it is not reported in the graph. The numbers around the matrix represent the the setup labels in short form (e.g., 1 stands for BLK360_3503964_Setup1).

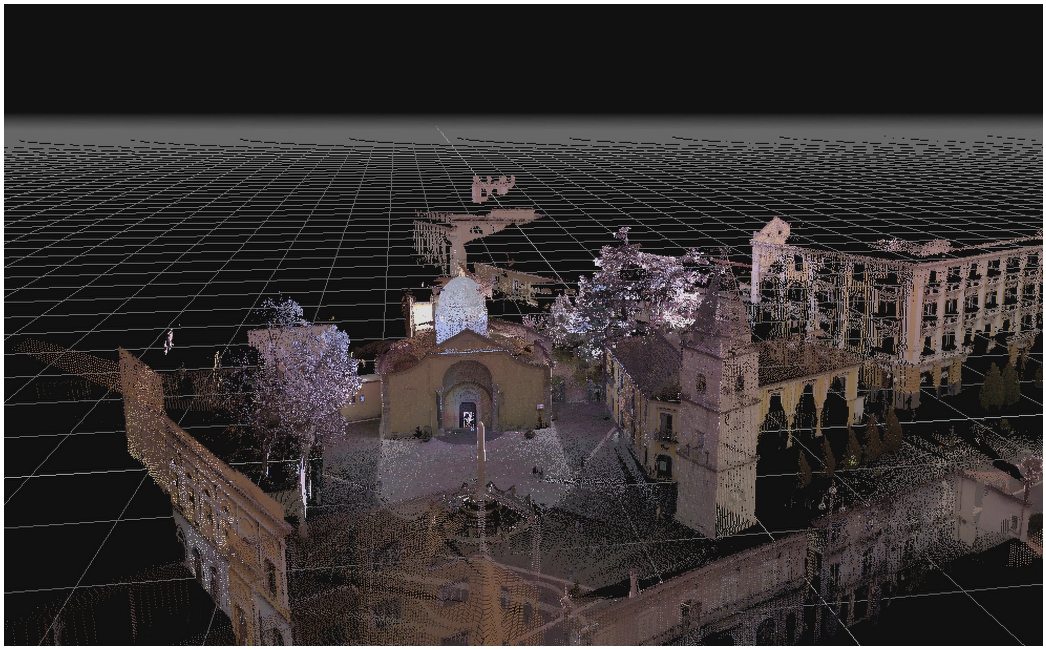

Figure 6. A view of the point cloud obtained by combining data from 32 setups. Note that in order to survey the façade, side walls and exterior of the apses, the laser scanner was placed at 11 locations outside the church, thus leading to the acquisition of data on the fountain, square and bell tower as well as some useless data on other surrounding buildings.

3.4. Solid Modeling

The bundle point cloud contained data representing the church from inside and outside. Specifically, the interior was fully surveyed, while the exterior contained a partial view of the church (façade and side walls, up to the gutter line), the square with the fountain and bell tower, and the façades of surrounding buildings. The roof of the church was missing, as the survey was made from the ground. Likewise, some parts of the church remained in the shadow cone of others.

After the cloud was cleaned to remove unnecessary parts by using 3DF Zephyr Free [46], the remaining points referred to a multiconnected three-dimensional domain with the exterior boundary surface not fully documented. As a consequence, an automatic reconstruction of the whole church appeared not possible, or at least not a very easy task.

However, from the point cloud measurements, it was recognized that most of the church could be modeled by solids with easy-to-draw boundary surfaces, such as planes for most of the façade (Figure 1a). In addition, the solid modeling of the church was not affected by the lack of data in the cloud. In fact, as can be seen from the aerial photographs (Figure 7), the missing part could be covered by flat patches, as in the case of the tiburium, which is bounded by six planes, or by patches with zero curvature in one direction, as in the case of the apses, which are bounded by portions of cylindrical surfaces (Figure 1b), or the roof. The latter can be subdivided into several regions, each of which can be seen as a neat, wavy surface in a predetermined direction, to roughly simulate the pattern of tiles, neglecting irrelevant details (see the enlarged box in Figure 7).

In addition, the three apsidal lunettes and the dome covering the tiburium were easy to model, being surfaces of almost perfect quarters of spheres and a half ellipsoid, respectively, as was ascertained by appropriate sections of the point cloud.

Based on geometric compatibility arguments, the dimensions and slope of those patches were easily estimated by combining measurements taken directly from the point cloud (such as the height and length of the gutter line, just to cite a few) with the results from typical tools of descriptive geometry, such as the rules of perspective and axonometry, which are useful for making fast, affordable and reliable by-hand estimations, and are not just out-of-date old-school techniques, even in the information technology era.

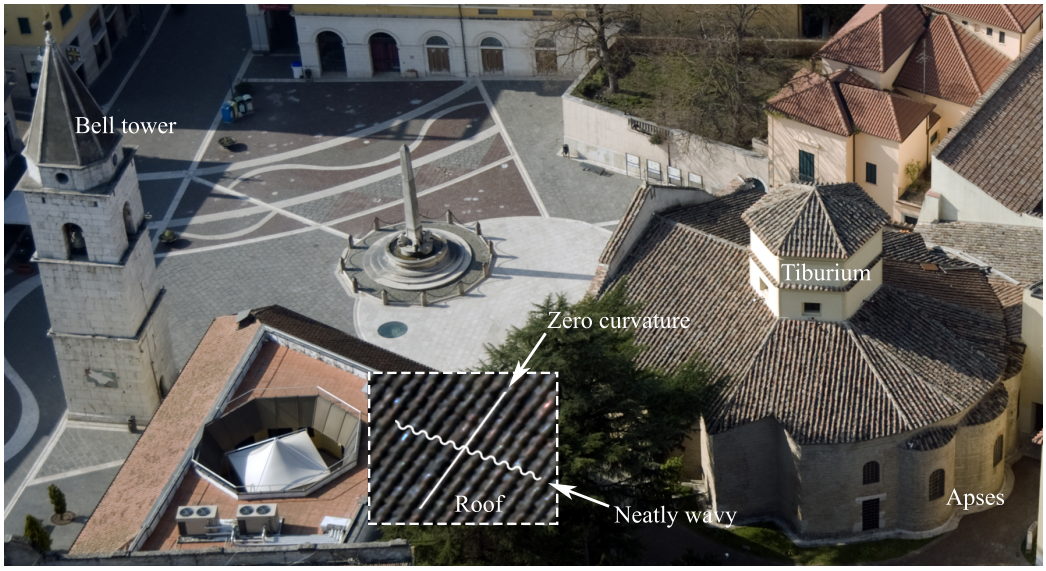

Figure 7. An aerial photograph allowing the addition of information lacking from the point cloud, such as the roof shape.

Descriptive geometry, in fact, provides insights into the spatial properties of 3D objects through 2D views, with a scientific approach that is certainly helpful for improving the use of modeling software as well [47].

This part of the work was performed using AutoCAD® software [48], for loading the point cloud into the workspace. Using it as a reference template, it was possible to reconstruct lines and section surfaces, and then obtain solids by extrusion. The resulting 3D solid model included almost all the details necessary to be used in documentation or analysis, apart the system of vaults, whose management required more sophisticated tools, as described in Section 4. We must, however, take into account that models are by definition abstractions and simplifications, and as such, something is left out because it is unknown or because it would provide unnecessary detail given the purpose of the model [49]. In the present case, fine details, although still very important in historical and archeological terms, were skipped if they were not relevant to the definition of the geometric properties of the church or their size was below the adopted scanner resolution. In a survey taken from the ground level, as in the present case, just increasing the resolution would not fix the problem: it would allow the detection of more details, but would still leave some others shadowed, at a price of making the point cloud uselessly large. Therefore, for a fully documented set of raw data, the point cloud in the present contribution should be complemented with higher resolution point clouds containing specific details, in a hierarchically multiresolution fashion [50], possibly aggregating data from different techniques and technologies, such as, for instance, using measurements from a robotized, lightweight, continuously rotating laser scanner mounted on micro-aerial vehicles allowing a high resolution in the near vicinity of the robot and a lower resolution with increasing distance from it [51].

With the already mentioned limits of the raw data, the 3D model with vaults but stripped of fine details and without the rendering of surfaces was useful for our primary research goal; that is, recognizing the geometric relationships among the parts to gain insights about the various configurations the church had in the past which are largely lost.

Nevertheless, it did not provide a sufficiently realistic representation suitable for the secondary goal; that is, dissemination to the general public. Indeed, the latter would predictably judge any virtual reconstruction of Santa Sofia as very poor if it was untextured and lacking in capitals, whose size were easily detected by the cloud, while their refined geometry was not. This would indeed nullify the potentialities of the models in the dissemination.

To overcome this drawback, the capitals were modeled using a reference-based approach, where overall measures (capital height and width) were taken from the point cloud,

while the appearance came from photographs since we did not scan the capitals at an adequate resolution because it was impossible from the ground.

To draw the capitals, taking advantage of the vertical planes of symmetry, it was sufficient to work on a single eighth of the reference capital, then mirrored to form the entire solid and appropriately scaled to fit the dimensions of the actual capitals in the church. Therefore, the final 3D model of each capital was just an approximation.

In addition, textures built from pictures taken inside and outside the church were applied to the solid by using manual unwrapping in SketchUp [52] (see Appendix A for details), and picture-quality rendering and real-time animations were made with OneRay-RT [53]. The animations were then combined and edited with the Animotica application [54] to obtain a short movie which also contained background royalty free music [55] and a narrator voice [56], explaining the history of Santa Sofia through its archeological phases, going back from the present day to the foundation of the church. This product is actually in line with the idea that short videos can be of help in presenting the relevant information about a monument, in a communicative manner suitable for a nonexpert audience, both adults and children [57]. In fact, a digital container allows new channels of knowledge to be opened up, enabling data to be linked and corrected quickly and a given topic to be fully and effectively communicated [58].

However, to avoid giving a false sense of reality, it is mandatory to warn the target users of the limits of the models. Indeed, the realism that a visualization may achieve could lead the users to perceive a virtual model as the truth instead of a perfectible model of reality, the level of accuracy of which depends on the field data available at the time the virtual reconstruction is made. This is true both for parts or objects that still exist and for those that have been lost, so it is necessary to emphasize the fact that 3D reconstructions may not reflect reality, instead being the result of interpretation.

Therefore, any virtual reconstruction should adequately state the level of authenticity that allows one to distinguish what is real from what is approximated or interpreted. This is a keenly felt issue, to the point that many archeologists have criticized the use of the term "reconstruction" itself; 3D models are tools for a better understanding of the past and not statements of reality [3,59].

However, these aspects, as well as the description of the part of the work that goes beyond the analysis carried out to reconstruct the geometry of the church's vaulting system, which this paper is actually aimed at, are left out in what follows. Finally, for completeness, a brief discussion on the reliability of 3D reconstructions is reported in Appendix B.

4. Approximation and Reconstruction of Vaults

4.1. Workflow of the Reconstruction of the System of Vaults

To reconstruct the 22 vaults covering the ambulacra of Santa Sofia, we considered a precise workflow that involved the use of different tools and steps that can be summarized as follows:

i. With 3DF Zephyr Free, the parts of the bundle point cloud containing only the vaults were selected;
ii. Data were exported on an ASCII `dat` file as 22 lists, one for each vault, containing 3D vectors (the coordinates of points);
iii. The `dat` file was loaded into *Mathematica* to compute the approximating surfaces;
iv. The resulting vaults were exported in a DXF™ file;
v. The file was inserted in the 3D models with AutoCAD®.

The core step in the process was the third one, and actually, it also involved a large number of operations, requiring the implementation of a trial-and-error loop-based approach.

In Table 1, it is detailed as a meta-code, which is written as a merely straight structured sequence of instructions, without reference to any specific programming language, for the sake of readability and generality.

To do this, general coding concepts are used, but the names of the instructions, i.e., `COMPUTE`, `DO`, `END`, `IF`, `SET`, `WHILE` written in teletype font (sometimes called typewriter font or monospace), may or may not correspond to those actually used in a specific programming language. However, the name and location of any instruction should make its meaning clear in the meta-code. In addition, there are also some comments in quotation marks that refer to the parts of the paper where more details can be read.

Table 1. The meta-code for the reconstruction of the vault surfaces.

Vault reconstruction from data	
`DATA`	
`SET` N;	"number of vaults, is a positive integer"
`SET` δ, ϵ;	"are positive real numbers"
`SET` u_1, u_2;	"are real numbers"
`IMPORT dat file`;	"the file of point coordinates is read here"
`BEGIN`	
`COMPUTE` $\mathbf{u} = (u_1, u_2, 0)/\sqrt{u_1^2 + u_2^2}$;	"is a horizontal unit vector"
100 `WHILE` $(j < N + 1)$ `DO`	
`COMPUTE` $\mathcal{S}_j^D$;	"surface through Delaunay triangulation, see e.g., [60]"
`CHECK` the quality of $\mathcal{S}_j^D$;	"see e.g., [61]"
200 `IF` the quality check is satisfied `THEN`	
$\mathcal{S}_j^\star \leftarrow \mathcal{S}_j^D$;	"the jth vault is stored and the code jumps to label 700"
`ELSE`	
`COMPUTE` the projection of the points of the jth vault on the floor;	
`COMPUTE` $\delta_{\max}$;	"diameter of the circle containing the projected points"
300 `WHILE` (error $> \epsilon$) `DO`	"see Equation (13)"
`COMPUTE` $M = \delta_{\max}/\delta$;	"the number of patches"
400 `WHILE` $(k < M + 1)$ `DO`	
`COMPUTE` $\mathcal{S}_j^D \cap \Pi_k^\delta$;	"Π_k^δ : kth $\mathbf{u}$–parallel vertical plane"
`COMPUTE` $\mathcal{S}_j^D \cap \Pi_{k+1}^\delta$;	"Π_{k+1}^δ is δ–shifted w.r.t. Π_k^δ"
`COMPUTE` the patch $P_k(x, y)$;	"see Sections 4.2 and 4.3"
500 `END WHILE`	"this closes `WHILE` loop at label 400"
`COMPUTE` $\mathcal{S}_j^C \leftarrow \bigcup_{k=1}^M P_k$;	"this returns a surface of patches"
`COMPUTE` the error;	"see Equation (12)"
$\delta \leftarrow \delta/2$;	"this halves δ to decrease the error in the next round"
600 `END WHILE`	"this closes `WHILE` loop at label 300"
700 `END IF`	"this closes `IF` at label 200"
`COMPUTE` $\mathcal{S}^\star \leftarrow \mathcal{S}^\star \bigcup \mathcal{S}_j^\star$;	"append the new vault to the list"
900 `END WHILE`	"this closes `WHILE` loop at label 100"
`END`	

As already stated, the actual code used to obtain the results that are shown in Section 5, was implemented in *Mathematica*. By taking advantage of the possibilities of such a high-level, general-purpose programming environment, the code was actually written with slightly different and more compact coding, resulting in more efficiency, but, however, being possibly less self-explanatory than the meta-code above.

4.2. Surface Approximation

As shown in Section 4.1, in terms of a meta-code, the *Mathematica* code is implemented in such a way that it, at first, approximates the jth vault, $j = \{1, \ldots, N\}$, in a system made of N vaults, with the surface $\mathcal{S}_j^D$, which is a Delaunay triangulation (or mesh) [60–62]. Such a mesh is computed by exploiting built-in functions. Only in the case where $\mathcal{S}_j^D$ fails to satisfy the mesh quality checks [63], an iterative procedure is activated and M patches $P_k(x, y)$, $k = 1, \ldots, M$, are constructed to approximate M subsets of points of the jth vault. The integer M is linked to both the overall dimensions of the vault projection, concisely characterized through the diameter $\delta_{\max}$ of the circle circumscribing the projected points,

and a given approximation length δ. Hence, the iterative procedure builds the surface approximation $\mathcal{S}_j^C$ joining M patches. To give further detail about the rules behind the construction of a single patch in the simplest way possible, we assume here that $\delta = \delta_{\max}$ and $M = 1$. Therefore $S_j^C \equiv P_1(x, y) = P(x, y)$.

Let us consider the surface of a quadrilateral vault and call the platform its projection on the floor (or any plane orthogonal to the direction of gravity). The platform, which is a general quadrangle, will be indicated with $\mathcal{P}$ from now on. Assigned a Cartesian frame of reference with origin O and axes x, y and z, we call $z = \mathcal{S}(x, y)$, $x, y \in \mathcal{P}$ the surface to be approximated. We assume $\mathcal{S}$ is sufficiently regular to admit a tangent plane everywhere.

As carried out above, let us call $P(x, y)$ the surface approximating $\mathcal{S}(x, y)$, and require that P exactly meets $\mathcal{S}$ at the boundary.

Therefore, if the four boundary curves, b_i, $i = \{1, \ldots, 4\}$, of the vault are known, they can be exploited to build P. However, writing functions $P(x, y)$ with $x, y \in \mathcal{P}$ can be a complicated task, which is made simpler if $\mathcal{P}$ is remapped on a unit square.

To fix the ideas, we assume, without loss of generality, that a side of $\mathcal{P}$ lies on the axis x (Figure 8a) and draw a reference grid, which is not conformal, in general. Such a grid is used to establish a bijective mapping $(x, y) \leftrightarrow (u, v)$ [64] from $\mathcal{P}$ to the unit square in the Cartesian reference frame $O'uv$ (Figure 8b).

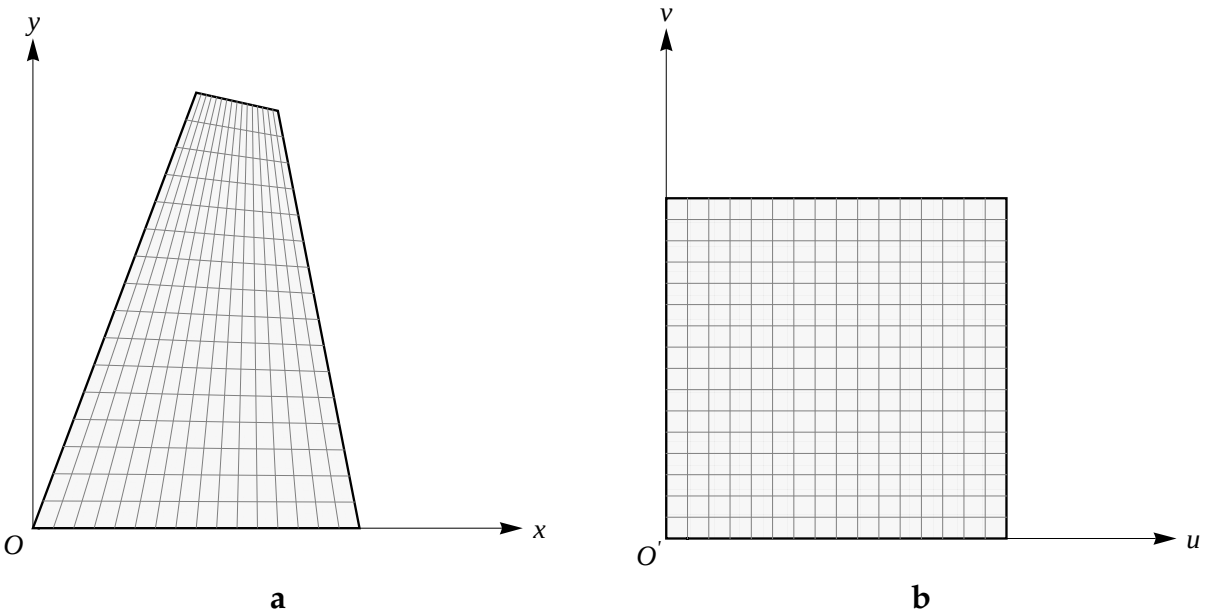

Figure 8. Reference grids: on the platform of the real vault (**a**) and on the unit square (**b**).

In Figure 9, three examples, a concave vault (left column, a), a tapered vault (middle column, b) and a saddle (right column, c), are shown.

In the mapping process $(x, y) \rightarrow (u, v)$, the curves b_i, $i = \{1, \ldots, 4\}$, which we assume to be the *real* edges of the vault (or surface) to be drawn (Figure 9, top panels), are remapped on the curves b_i', $i = \{1, \ldots, 4\}$ (Figures 9, second line of panels from the top), which are simpler to write and are used to build the function $P(u, v)$ (Figure 9, second line of panels from the bottom).

By exploiting the inverse mapping, $(x, y) \leftarrow (u, v)$, $P(x, y)$, which we assume to be the graphics of the *real* vault (or surface), is finally obtained (Figure 9, bottom panels).

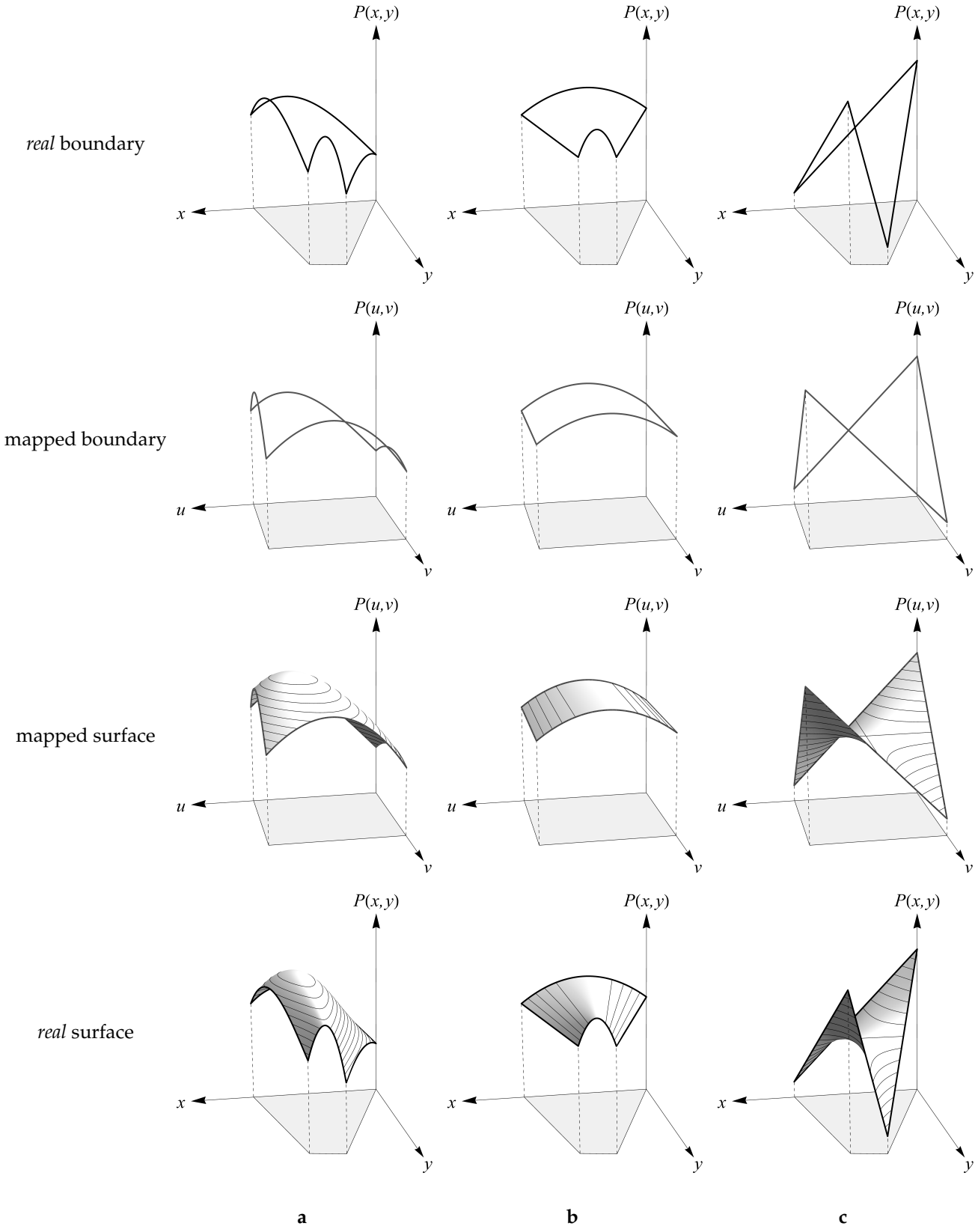

Figure 9. Surfaces from boundary edges: a concave vault (column **a**), a tapered vault (column **b**) and a saddle (column **c**).

4.3. Patch Construction on the Unit Square Domain

The functions b'_i, $i = \{1, \ldots, 4\}$ can be put in analytic form through selected shape functions using as control parameters the ordinates h_r (height parameters) and the local derivatives s_r (slope parameters), $r = \{0, 1\}$, of b'_i evaluated at the boundaries of their domain spanning from 0 to 1. Assigned a certain dummy variable $0 \leq t \leq 1$ and choosing the Hermite cubics, $H_n(t)$, $n = \{1, \ldots, 4\}$, as shape functions, $b'_i(t)$ takes the form

$$b'_i(t) = h^i_0 H_1(t) + h^i_1 H_2(t) + s^i_0 H_3(t) + s^i_1 H_4(t)\,, \tag{1}$$

where

$$H_1(t) = f(t)\,, \tag{2}$$
$$H_2(t) = f(1-t)\,, \tag{3}$$
$$H_3(t) = g(t)\,, \tag{4}$$
$$H_4(t) = -g(1-t)\,, \tag{5}$$

with $f(t)$ and $g(t)$ third-degree polynomials defined as

$$f(t) = (1+2t)(1-t)^2\,, \tag{6}$$
$$g(t) = t(1-t)^2\,. \tag{7}$$

The graphs of $H_n(t)$, $n = \{1, \ldots, 4\}$, are shown in Figure 10.

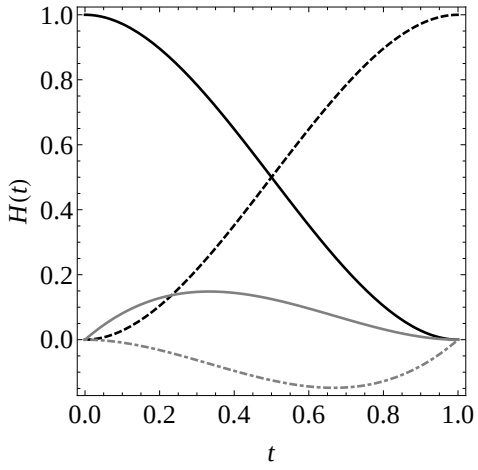

Figure 10. Hermite functions $H_1(t)$ (solid black), $H_2(t)$ (dashed black), $H_3(t)$ (solid gray), $H_4(t)$ (dot–dashed gray).

We note that the functions obtained by intersecting the approximating function $P(u, v)$ with the vertical planes passing through the sides of the unit square ($v = 0$, $v = 1$, $u = 0$, and $u = 1$) are $b'_1 = P(u, 0)$, $b'_2 = P(u, 1)$, $b'_3 = P(0, v)$ and $b'_4 = P(1, v)$, and the values of $P(u, v)$ at the four corners coincide with the parameters appearing in Equation (1), i.e., the height parameters such as, e.g., $P(0, 0) = h^1_0 = h^3_0$, $P(1, 0) = h^1_1 = h^4_0, \ldots$, and the slope parameters such as, e.g., $P_{,u}(0, 0) = s^1_0$, $P_{,v}(0, 0) = s^3_0, \ldots$, where the comma notation for partial derivatives

$$P_{,\alpha}(u^\star, v^\star) = \left.\frac{\partial P}{\partial \alpha}\right|_{\substack{u=u^\star \\ v=v^\star}} \tag{8}$$

is exploited for ease of notation. The choices made lead us to basically use bicubically blended Coons patches [19] defined on the unit square (see also [65], for details on Coons surfaces and their applications).

By defining the vector $\mathbf{F}(t)$ as

$$\mathbf{F}(t) = (H_1(t), H_2(t), H_3(t), H_4(t)), \tag{9}$$

with t being u or v, and the matrix $\mathbf{P}$ as

$$\mathbf{P} = \begin{pmatrix} P(0,0) & P(0,1) & P_{,v}(0,0) & P_{,v}(0,1) \\ P(1,0) & P(1,1) & P_{,v}(1,0) & P_{,v}(1,1) \\ P_{,u}(0,0) & P_{,u}(0,1) & P_{,uv}(0,0) & P_{,uv}(0,1) \\ P_{,u}(1,0) & P_{,u}(1,1) & P_{,uv}(1,0) & P_{,uv}(1,1) \end{pmatrix}, \tag{10}$$

the approximating surface is obtained as

$$P(u,v) = \mathbf{F}^T(u)\mathbf{P}\mathbf{F}(v). \tag{11}$$

Recalling what was stated above, the entries of Equation (10) $P(i,j)$, $P_{,u}(i,j)$, $P_{,v}(i,j)$, $P_{,uv}(i,j)$ stand for the values of $P(u,v)$ and its first and mixed second partial derivatives evaluate at u and v, which take values 0 or 1.

Hence, by assigning four edges that properly meet at the corners to approximate the patch, only the mixed second derivatives of $P(u,v)$, usually addressed as the twists, are unknowns. Since we are not able to provide twists in advance, we assume in the following that the twists at the corners are null. Such a choice automatically guarantees the C^1 continuity of a surface made with a network of patches, although it may present drawbacks, as is emphasized in [19].

4.4. Error Estimate

The results obtained using any mathematical model designed to characterize certain objects of interest will contain errors, independently of the appropriateness of the model itself [66]. It is therefore mandatory to evaluate the quality of the calculated solutions. In addition, the error estimate also allows for improved approximation in the iterative search for solutions.

Recalling that the generic point p in the cloud can be expressed as a position vector $\mathbf{p} = (x_p, y_p, z_p)$ with $z_p = p(x_p, y_p)$, we assume here that the approximation error can be related to an appropriate comparison of z_p with the height of the patch P at the same coordinates x_p and y_p, i.e., $z_P = P(x_p, y_p)$.

Therefore, neglecting subscripts for ease of notation, to evaluate the quality of the approximation in a dimensionless way, we consider the absolute value of the relative error (ARE), defined as

$$\mathrm{ARE}(x,y) = \left| \frac{P(x,y) - p(x,y)}{p(x,y)} \right|, \tag{12}$$

and accept approximations satisfying the inequality

$$\mathrm{ARE}(x,y) \leq \epsilon \qquad \forall (x,y) \in \mathcal{P}, \tag{13}$$

where ϵ is a positive real number to be chosen. The smaller ϵ is, the closer the approximate surface is to the points of the cloud.

It is worth noting that Equation (12) is of course not the only possible formula for error estimation. Indeed, many different a posteriori error estimates can be designed with respect to user-defined quantities of interest, and virtually all available approaches give useful information on the quality of computed solutions [67].

5. Results

Following the procedure shown in Section 4, the parts of the point cloud containing only the vaults (Figure 11a) were meshed with a Delaunay triangulation (Figure 11b). While the quality requirement of the triangulation produced polyhedral surfaces, which were

satisfactory on the most part of the vault domains, the noise in data produced unsatisfactory approximation close to the boundaries; therefore, the meshes did not pass the quality test, and to overcome such a drawback, the smooth approximation of the polyhedral surfaces through Coons patches was used.

As shown in Section 4.3, it is possible to construct a surface by writing the parametric representation of the curves approximating the boundary data of an entire vault.

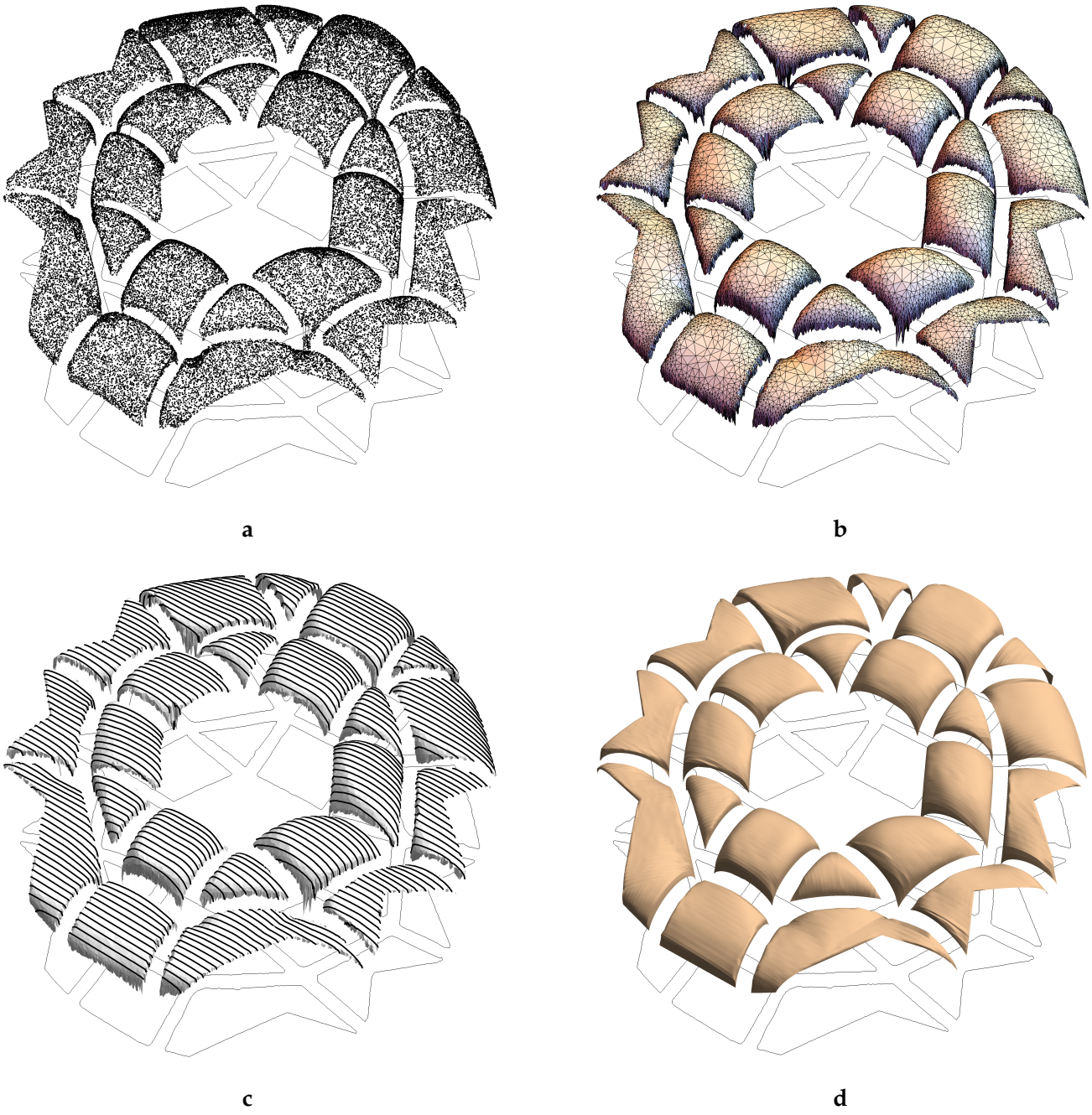

Figure 11. Point cloud of the system of vaults (**a**); Delaunay triangulation of the point cloud (**b**); superimposition of section lines to the triangulated surface (**c**); smoothed vault surface (**d**).

However, in the general case, this does not guarantee that the obtained patch will be a good approximation of the vaults itself. Therefore, the slicing of the vaults (Figure 11c), following the strategy shown in the meta-code reported in Table 1, improved the approximation (Figure 11d). In addition, with the way that real vaults are made, choosing on the domain of the platforms strips thin enough to have both the curves on the long edges and

the curves on the short edges almost parallel to each other, any approximating function would resemble a translational surface. As these kinds of surfaces are characterized by the vanishing twist everywhere, problems associated with our choice of zero twist at the corners of the unit square were mitigated.

The values of the adopted estimator $\mathrm{ARE}(x, y)$ given by Equation (12) are graphically shown in Figure 12a, along with their distribution, ordered from the lowest to the largest value, versus the dimension of the dataset (Figure 12b).

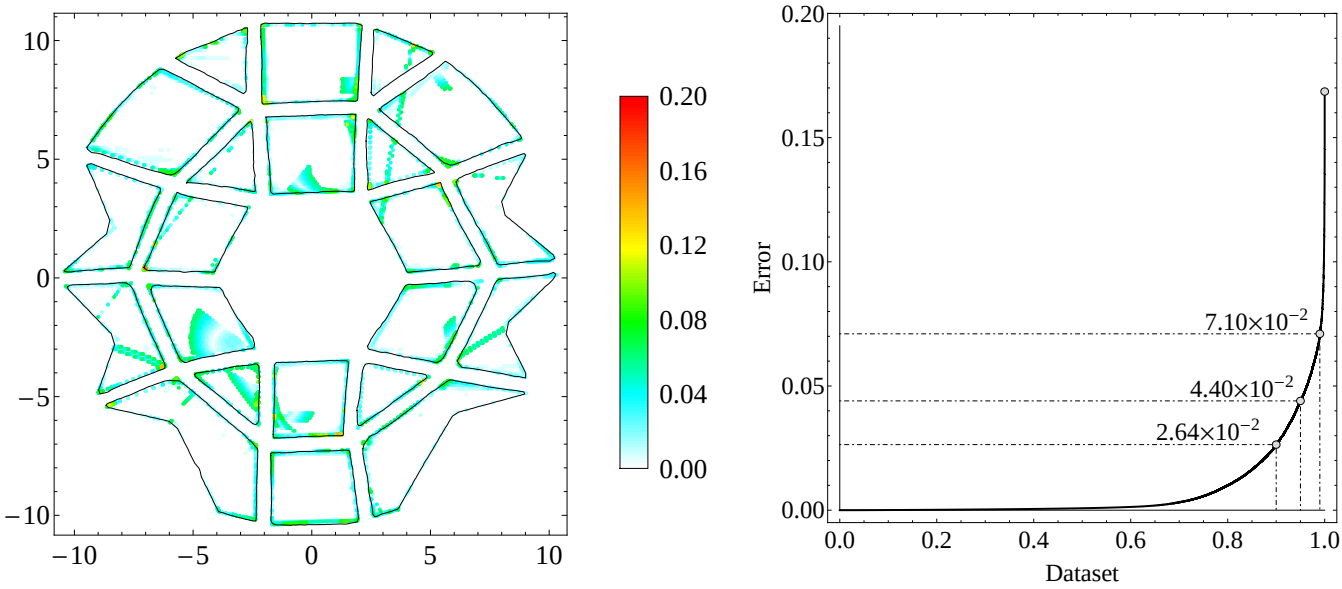

Figure 12. Color map of $\mathrm{ARE}(x, y)$ (**a**) and its ordered distribution versus the dataset (**b**).

Indeed, it can be observed that the relative error remained low for the majority of the reference domain. Specifically, Figure 12b demonstrates that the error took values below 2.64 % for 90 % of the data. However for 5 % of the data, it exceeded 4.40 %, and for only 1 % of the data, it surpassed 7.70 %, with a maximum value of 16.85 %.

Based on these results, the approximation shown in Figure 11d was judged satisfactory.

In agreement with the steps (iv) and (v) of the workflow reported in Section 4.1, once the surface reconstruction process performed with *Mathematica* was completed, the resulting vaults were exported as a DXF™ file to be managed in AutoCAD® and inserted in the 3D model.

The remaining steps were briefly described in Section 3.4. However, further details on them are beyond the scope of this contribution, as stated there.

Finally, in Figures 13 and 14, the rendered results are shown, mainly to enlighten the complex geometry of the system of vaults of Santa Sofia and to emphasize that while it certainly produces a meditative and prayerful environment in the real world, it also offers mathematical and modeling complications that require the specifically tailored tools adopted in the present study.

Some Remarks about the Approach

The availability of software that automatically produces a 3D model from a point cloud via surface meshes could generate the mistaken belief that a certain model is the only logical outcome of a survey. More properly, such a model would correspond to one among those mathematically compatible with the points acquired in the scan. Consequently, meshing with different algorithms may obviously yield different results [68].

Indeed, there are many software able to generate meshes, with arbitrary levels of quality and accuracy, such as MeshLab [69,70], and also that are suitable to perform the

so-called retopology, which is the process of simplifying the topology of a mesh (see, e.g., Blender [71], gSculpt [72], or ZBrush [73], to cite a few).

In particular, retopology could be applied to the Delaunay triangulation constructed with *Mathematica* to make it smoother. However, retopology is a complex process, still largely unsolved, that focuses on extracting quad meshes based on the shape of the input mesh, rather than on what the input is and what uses will be made of it once it is remeshed [74].

Figure 13. A rendered view of the interior of the church showing the complex structure of the vaults covering the inner and outer ambulacra. Remains of early medieval frescoes are visible on the apsidal basins [34].

Figure 14. A rendered view of the tiburium and its ellipsoidal dome, taken from below.

In addition, the rationale for the approach we consider here compared to directly exploiting the built-in approximation functions in AutoCAD® (where Coons patches are actually implemented as well) after the slicing process is performed, is based on the need to keep the approximation error below a desired threshold, which we can decide in advance.

Therefore, to maintain control of all the terms appearing in the approximation, the solution proposed in Section 4 appears to be the most suitable for the scopes of the research project we are dealing with. Furthermore, it enables us to directly extend the code by using the typical tools of differential geometry [75], which as well as being important in computational graphics, also play a relevant role in mechanics and structural analysis (for instance, the components of the curvature tensor are relevant in the analysis of the folding of surfaces under compression [76] or the equilibrium of vaults and domes [77]).

In fact, having full control also allows us to design steps in the direction of structural analysis, which of course is equally important for heritage protection and, in particular, for studying the behavior of masonry vaults through the development of appropriate finite element meshes [18].

6. Conclusions

The present paper gives an account of the methodology used to analyze and virtually reconstruct some archeological and architectural phases of Santa Sofia in Benevento. The reconstruction, in terms of 3D modeling, presented stages of very different levels of difficulty. Indeed, some parts of the church present shapes that are very easy to draw, while others do not resemble any basic primitive geometry and required specific analysis. Therefore, to reconstruct the complex system of vaults covering the two ambulacra, a home-made code based on remapping Coons patches was written.

The 3D model of Santa Sofia is an example of virtual heritage. By this designation, which is widespread in the field of cultural heritage, the use of 3D digital representations of monuments or archeological sites in the various configurations of the past is conventionally defined. Three-dimensional representations are the synthesis of research, expressed visually, and can be considered the natural development of traditional graphic techniques or plastic models, but unlike such reproductions, digital graphics are much more flexible because they allow for easy modifications. For example, as new data are discovered through archeological campaigns, archeometric investigations of masonry or new exegesis of sources, the new information can be added more easily, yielding naturally updated results that can be implemented in or improve the reconstruction.

Finally, ease of transmission and communication distinguishes 3D graphics products because their digital nature inherently allows for replicability by facilitating their dissemination to a nonexpert audience and sharing to the scientific community.

Author Contributions: Conceptualization, methodology, writing and visualization, E.B. and S.R.; solid 3D modeling and software development, E.B.; data curation, texturing and rendering, S.R. All authors have read and agreed to the published version of the manuscript.

Funding: This research received no external funding.

Data Availability Statement: The original contributions presented in the study are included in the article. Any further inquiry can be directed to the authors.

Acknowledgments: The authors would like to thank Marcello Rotili for the helpful discussions on the topics covered in the article. E.B. dedicates this work to the memory of his beloved mother Maria Domenica Maio (16 June 1944–21 January 2021).

Conflicts of Interest: The authors declare no conflict of interest.

Appendix A. SketchUp UV Mapping

The modeling process of projecting a certain surface of a 3D model to a 2D image for texture mapping is known as UV mapping, where U and V denote the axes of the 2D texture, while X, Y and Z are often used to denote the axes of the 3D object in model space. In SketchUp, to display unfolded UV faces of the surface of the model, *Edit UVs* can be used and the tools *Move*, *Rotate* and *Scale* allow the UV faces to be adjusted to match the desired texture placement. To apply textures to the 3D models, the manual UV unwrapping can be used through the steps summarized as follows:

i. Select the model to apply a texture on;
ii. Select *Position Texture*, allowing to manually position and scale the texture on the surface of the model;
iii. Select *Apply* button to map the texture onto the model.

Although more time-consuming if compared to the automatic unwrapping also available in SketchUp, the manual unwrapping offers more control and precision. Therefore, it is suitable for complex models or for the placement of a specific texture.

Appendix B. Reliability of 3D Reconstructions

Here we present the methodology adopted to assess the reliability of the 3D reconstructions of the five main archeological phases of the church of Santa Sofia; three of these are represented in Figure 3.

The graph shown in Figure A1 summarizes, in a matrix fashion, the elements that enabled the reconstructions, i.e., archeological evidences, information about architectural elements and the methodologies for the interpretation and integration of missing data.

By grading the availability of information on a scale spanning from absent data to fully available, one can obtain an overall assessment of the validity of the hypotheses and reconstruction results.

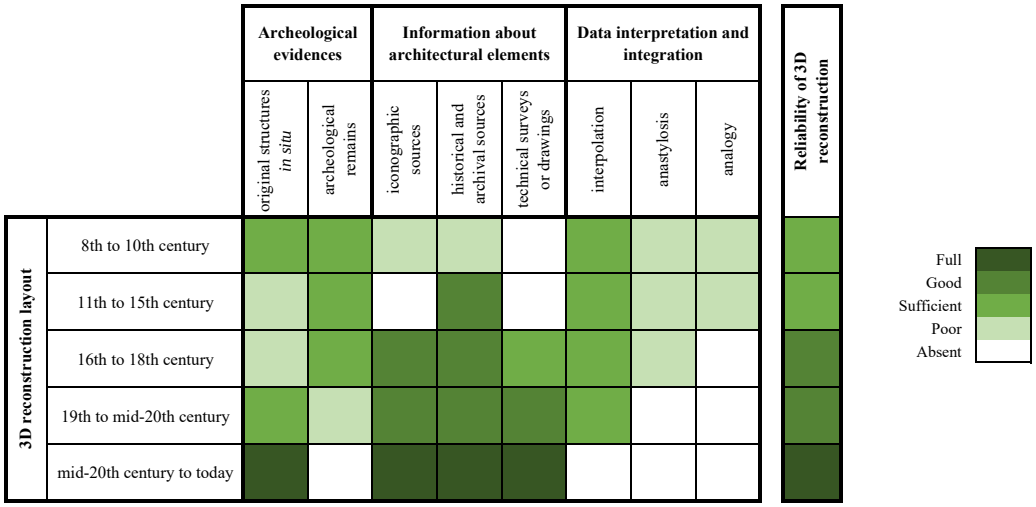

Figure A1. Reliability matrix of 3D reconstructions.

According to [78], the methodologies used in the integration of data for reconstructions are commonly based on:

i. Interpolation: a process similar to gap filling, which allows two distant elements to be reconnected through an "interpolation";
ii. Anastylosis, which consists of recomposing the parts of a monument using software in which the surveyed elements, preferably in 3D, have to be repositioned in their original location;
iii. Analogy, which allows an apparatus that is coherent with the studied object to be reconstructed, in terms of architectural and stylistic language, through similarity matches between the attested and documented elements.

All these approaches were applied in the present study, with different levels of use.

References

1. Pfarr-Harfst, M.; Grellert, M. The reconstruction—Argumentation method. In Proceedings of the Digital Heritage. Progress in Cultural Heritage: Documentation, Preservation, and Protection, Nicosia, Cyprus, 31 October–5 November 2016; Ioannides, M., Fink, E., Moropoulou, A., Hagedorn-Saupe, M., Fresa, A., Liestøl, G., Rajcic, V., Grussenmeyer, P., Eds.; Springer International Publishing: Cham, Switzerland, 2016; pp. 39–49.
2. Antuono, G.; Cundari, M.R.; Cundari, G.C.; Bagordo, G.M. Survey, data analysis and modeling Raphael's Stables in Villa Farnesina, Rome. *Heritage* **2023**, *6*, 4243–4262. [CrossRef]
3. Pietroni, E.; Ferdani, D. Virtual restoration and virtual reconstruction in Cultural Heritage: Terminology, methodologies, visual representation techniques and cognitive models. *Information* **2021**, *12*, 167. [CrossRef]
4. Rotili, M. *Benevento Romana e Longobarda. L'immagine Urbana*; Banca Sannitica: Napoli, Italy, 1986.
5. Rotili, M. La chiesa di Santa Sofia a Benevento. In *Benevento. Le Chiese del Fondo Edifici di Culto del Sannio*; Edizioni L'Orbicolare: Milano, Italy, 2011; pp. 27–48.
6. Rotili, M. Arechi II e Benevento. In *Tra i Longobardi del Sud*; Rotili, M., Ed.; Il Poligrafo: Padova, Italy, 2017; pp. 181–226.
7. Rotili, M. Benevento, chiesa di Santa Sofia. Le vicende storiche e architettoniche. In *Sulla Pittura Beneventana, Aggiornamento Scientifico*; Bertelli, G., Mignozzi, M., Eds.; Mario Adda Editore: Bari, Italy, 2021; pp. 79–82.
8. Arrighetti, A.; Pansini, R. Introduction [Introduzione]. *Archeol. e Calc.* **2022**, *33*, 9–14. [CrossRef]
9. Gabellone, F. *Archeologia Virtuale: Teoria, Tecniche e Casi di Studio*; Edizioni Grifo: Lecce, Italy, 2019.
10. Rotili, M.; Rapuano, S. Le ricerche nel castello e nell'area murata del Monte (1980–1992; 2005–2007): Divulgazione e valorizzazione. In *Archeologia Pubblica, Paesaggi e Culture, e Innovazione Sociale. Alcuni Casi di Studio in Campania e Molise. Studi in Onore di Giuseppina Bisogno e in Ricordo di Carmine Diglio*; Senatore, A., Mancini, R., Albini, A., Scaduto, M.L., De Tommasi, A., Eds.; All'Insegna del Giglio: Sesto Fiorentino, Italy, 2022; pp. 69–82.
11. Fassi, F. 3D modeling of complex architecture integrating different techniques—A critical overview. *Int. Arch. Photogramm. Remote Sens. Spat. Inf. Sci.* **2007**, *XXXVI-5/W47*, 1–11.
12. Iannizzaro, V.; Barba, S.; Messina, B.; D'Agostino, P.; Fiorillo, F. The domes of the Amalfi Coast: Survey and digital representation of complex shapes. In Proceedings of the International Congress Domes in the World. Symbolism and Cultural Identity, Geometric and Formal Genesis, Construction, Identification, Conservation, Florence, Italy, 19–23 March 2012; Tampone, G., Corazzi, R., Mandelli, E., Eds.; Nardini Editore: Florence, Italy, 2012; pp. 1–12.
13. Capone, M.; Campi, M.; Catuogno, R. Gothic churches in Paris St Gervais et St Protais image matching 3D reconstruction to understand the vaults system geometry. *Int. Arch. Photogramm. Remote Sens. Spat. Inf. Sci.* **2015**, *XL-5/W4*, 423–430. [CrossRef]
14. Bevilacqua, M.G.; Caroti, G.; Martínez-Espejo Zaragoza, I.; Piemonte, A. Frescoed vaults: Accuracy controlled simplified methodology for planar development of three-dimensional textured models. *Remote Sens.* **2016**, *8*, 239. [CrossRef]
15. Brumana, R.; Condoleo, P.; Grimoldi, A.; Banfi, F.; Landi, A.G.; Previtali, M. HR LOD based HBIM to detect influences on geometry and shape by stereotomic construction techniques of brick vaults. *Appl. Geomat.* **2018**, *10*, 529–543. [CrossRef]
16. Murphy, M.; McGovern, E.; Pavia, S. Historic building information modelling (HBIM). *Struct. Surv.* **2009**, *27*, 311–327. [CrossRef]
17. Lanzara, E.; Samper, A.; Herrera, B. Point cloud segmentation and filtering to verify the geometric genesis of simple and composed vaults. *Int. Arch. Photogramm. Remote Sens. Spat. Inf. Sci.* **2019**, *XLII-2/W15*, 645–652. [CrossRef]
18. Angjeliu, G.; Cardani, G.; Coronelli, D. A parametric model for ribbed masonry vaults. *Autom. Constr.* **2019**, *105*, 102785. [CrossRef]
19. Farin, G. *Curves and Surfaces for CAGD: A Practical Guide*; Computer Graphics and Geometric Modeling; Elsevier Science: Amsterdam, The Netherlands, 2002.
20. Fregonese, L.; Adami, A. The 3D model of St. Mark's Basilica in Venice. In *Digital Transformation of the Design, Construction and Management Processes of the Built Environment*; Daniotti, B., Gianinetto, M., Della Torre, S., Eds.; Springer International Publishing: Cham, Switzerland, 2020; pp. 343–354. [CrossRef]
21. Spallone, R.; López González, M.C.; Vitali, M.; Bertola, G.; Natta, F.; Ronco, F. Recognizing the design patterns of complex vaults: Drawing, survey and modeling. Experiments on Palazzo Mazzonis' atrium in Turin. In Proceedings of the Digital Heritage. Progress in Cultural Heritage: Documentation, Preservation, and Protection, Virtual, 2–5 November 2020; Ioannides, M., Fink, E., Cantoni, L., Champion, E., Eds.; Springer International Publishing: Cham, Switzerland, 2021; pp. 3–14.
22. Incerti, M. Dal rilievo all'analisi di superfici complesse: il caso della pseudo-cupola di Galla Placidia. *Archeol. Calc.* **2022**, *33*, 55–72. [CrossRef]
23. Capone, M.; Palomba, D.; Scandurra, S.; Lanzara, E. Trapezoidal and apsidal ribbed vaults smart 3D reconstruction. *Int. Arch. Photogramm. Remote Sens. Spat. Inf. Sci.* **2022**, *XLVI-2/W1-2022*, 135–142. [CrossRef]
24. Jobbik, E.; Krähling, J. A self-contained stellar vault construction method. The vault of the Matthias Oratorio in the Inner City Parish Church of Budapest. *Period. Polytech. Archit.* **2023**, *54*, 73–85. [CrossRef]
25. Jobbik, E.; Krähling, J. A cross-vault system's relative periodisation based on geometric analysis: The vaulting system of the apse of the Inner City Parish Church of Budapest. *Építés-Építészettudomány* **2023**, *51*, 115–137. [CrossRef]
26. Wolfram Research, Inc. *Mathematica, Version 8.0*; Wolfram Research, Inc.: Champaign, IL, USA, 2010.
27. Complectens monumenta varia spectantia ad ecclesiam, monasterium et monachos Sanctae Sophiae, Volumen III. Ancient manuscript document. Currently housed in the Archivio Storico Provinciale di Benevento, Fondo S. Sofia, Benevento, Italy.
28. de Nicastro, G. *Benevento Sacro, a cura di Gaetana Intorcia*; Stabilimento Litotipografico Editoriale De Martini: Benevento, Italy, 1976.

29. Hourihane, C.P. *The Grove Encyclopedia of Medieval Art and Architecture*; Oxford University Press: Oxford, UK, 2012; Volume 1, p. 305.
30. Basile, S. Restauri settecenteschi a Benevento. *Samnium* **1970**, *43*, 184–189.
31. Zazo, A. La piazza e la fontana di S. Sofia in Benevento (1809). *Samnium* **1929**, *1*, 95–96.
32. I Longobardi in Italia. I Luoghi del Potere. Available online: https://www.unesco.it/it/PatrimonioMondiale/Detail/156 (accessed on 20 May 2023).
33. Carella, S. Sainte-Sophie de Bénévent et l'architecture religieuse longobarde en Italie méridionale. *Hortus Artium Mediev.* **2003**, *9*, 331–356. [CrossRef]
34. Belting, H. *Studien zur beneventanischen Malerei*; Forschungen zur Kunstgeschichte und christlichen Archäologie, Steiner: Tokyo, Japan, 1968; pp. 42–53.
35. Rusconi, A. Unpublished technical document. Currently housed in the Archivio della Soprintendenza Archeologia Belle Arti e Paesaggio per le province di Caserta e Benevento, Caserta (Italy).
36. Rusconi, A. La chiesa di Santa Sofia di Benevento. In *XIV Corso di Cultura sull'Arte Ravennate e Bizantina*; Longo Editore: Ravenna, Italy, 1967; pp. 339–359.
37. Ferrante, M. Chiesa e chiostro di Santa Sofia in Benevento. *Samnium* **1952**, *XXV*, 73–96.
38. Zazo, A. *Benevento*; Istituto S. Michele a Ripa: Rome, Italy, 1928.
39. Rotili, M. (Ed.) *Achille Vianelli: Catalogo della Mostra Celebrativa*; Gaetano Casella Editore: Napoli, Italy, 1954.
40. Parisi, R. Iconografia di una città pontificia: Benevento in età moderna e contemporanea. In *Iconografia delle Città in Campania. Le Province di Avellino, Benevento, Caserta e Salerno*; de Seta, C., Buccaro, A., Eds.; Electa Napoli: Napoli, Italy, 2007; pp. 173–194.
41. Fontana di SantaSofia a Benevento [Fountain of Santa Sofia in Benevento]. Watercolor, 19th century. Currently housed in the Museum of Sannio, Benevento (Italy).
42. Martin, J.M. *Chronicon Sanctae Sophiae: Cod. Vat. Lat. 4939*; Istituto Storico Italiano per il Medio Evo: Rome, Italy, 2000.
43. Leica Geosystems. Leica BLK360 Imaging Laser Scanner. Available online: https://leica-geosystems.com/products/laser-scanners/scanners/blk360 (accessed on 6 June 2023).
44. *853811-2.0.0en*; Leica BLK360 User Manual, Version 2.0. Leica Geosystems AG: Heerbrugg, Switzerland, 2017.
45. *Leica Geosystems QuickStart Guide*; Leica Geosystems AG: Heerbrugg, Switzerland, 2018. [CrossRef]
46. 3DFLOW. 3DF Zephyr Free. Available online: https://www.3dflow.net/3df-zephyr-free/ (accessed on 7 June 2023).
47. Stachel, H. The evolution of Descriptive Geometry in Austria. In *Descriptive Geometry, the Spread of a Polytechnic Art: The Legacy of Gaspard Monge*; Barbin, É., Menghini, M., Volkert, K., Eds.; Springer International Publishing: Cham, Switzerland, 2019; pp. 181–195. [CrossRef]
48. Autodesk, INC. AutoCAD®. Available online: https://www.autodesk.com/products/autocad (accessed on 7 June 2023). [CrossRef]
49. Clark, J.T. The fallacy of reconstruction. *Cyber-Archaeology* **2010**, *2177*, 63–73. [CrossRef]
50. Teruggi, S.; Grilli, E.; Russo, M.; Fassi, F.; Remondino, F. A hierarchical machine learning approach for multi-level and multi-resolution 3D point cloud classification. *Remote Sens.* **2020**, *12*, 2598. [CrossRef]
51. Droeschel, D.; Stückler, J.; Behnke, S. Local multi-resolution representation for 6D motion estimation and mapping with a continuously rotating 3D laser scanner. In Proceedings of the 2014 IEEE International Conference on Robotics and Automation (ICRA), Hong Kong, China, 31 May–7 June 2014; pp. 5221–5226. [CrossRef]
52. Trimble Inc. SketchUp Pro. Available online: https://www.sketchup.com/ (accessed on 7 June 2023).
53. AnalistGroup. OneRay-RT. Available online: https://www.analistgroup.com/it/software-rendering-3d (accessed on 7 June 2023).
54. Mixilab. Animotica. Available online: https://www.animotica.com/ (accessed on 7 June 2023).
55. FiftySounds. Tracks: *All That Reamins*, *Only the Braves*. Available online: https://www.fiftysounds.com (accessed on 7 June 2023).
56. Woord. Instant Text-to-Speech (TTS) Using Realistic Voices. Available online: https://www.getwoord.com (accessed on 7 June 2023). [CrossRef]
57. Ioannides, M.; Chatzigrigoriou, P.; Bokolas, V.; Nikolakopoulou, V.; Athanasiou, V.; Papageorgiou, E.; Leventis, G.; Sovis, C. Educational creative use and reuse of digital cultural heritage data for Cypriot UNESCO monuments. In Proceedings of the Digital Heritage. Progress in Cultural Heritage: Documentation, Preservation, and Protection, Nicosia, Cyprus, 31 October–5 November 2016; Ioannides, M., Fink, E., Moropoulou, A., Hagedorn-Saupe, M., Fresa, A., Liestøl, G., Rajcic, V., Grussenmeyer, P., Eds.; Springer International Publishing: Cham, Switzerland, 2016; pp. 891–901. [CrossRef]
58. Chiarenza, S.; Accardi, A.R.D.; Inglisa, R. Technological innovation and new presentation strategies for virtual museum exhibitions. *Int. Arch. Photogramm. Remote Sens. Spat. Inf. Sci.* **2019**, *XLII-2/W15*, 311–318. [CrossRef]
59. Ferdani, D.; Demetrescu, E.; Cavalieri, M.; Pace, G.; Lenzi, S. 3D modelling and visualization in field archaeology. From survey to interpretation of the past using digital technologies. *Groma* **2019**, *4*, 1–21. [CrossRef]
60. Shewchuk, J.R. Triangle: Engineering a 2D quality mesh generator and Delaunay triangulator. In Proceedings of the Applied Computational Geometry towards Geometric Engineering, Philadelphia, PA, USA, May 1996; Lin, M.C., Manocha, D., Eds.; Springer: Berlin/Heidelberg, Germany, 1996; pp. 203–222. [CrossRef] [PubMed]
61. Cazals, F.; Giesen, J. Delaunay triangulation based surface reconstruction. In *Effective Computational Geometry for Curves and Surfaces*; Boissonnat, J.D., Teillaud, M., Eds.; Springer: Berlin/Heidelberg, Germany, 2006; pp. 231–276. [CrossRef]

62. Khan, D.; Plopski, A.; Fujimoto, Y.; Kanbara, M.; Jabeen, G.; Zhang, Y.J.; Zhang, X.; Kato, H. Surface remeshing: A systematic literature review of methods and research directions. *IEEE Trans. Vis. Comput. Graph.* **2022**, *28*, 1680–1713. [CrossRef]
63. Du, Q.; Wang, D. Recent progress in robust and quality Delaunay mesh generation. *J. Comput. Appl. Math.* **2006**, *195*, 8–23. [CrossRef]
64. Wimmer, K.; Bauer, R.; Halama, S.; Hobler, G.; Selberherr, S. Transformation methods for nonplanar process simulation. *Simul. Semicond. Devices Process.* **1991**, *4*, 131–138. [CrossRef]
65. Chang, K.H.; Liu, F.; Ji, X.; Gao, J. Extended SQ-Coons surface and its application on fairing automobile surface design. *Math. Probl. Eng.* **2020**, *2020*, 4912978. [CrossRef]
66. Prudhomme, S. A Posteriori Error Estimates of quantities of interest. In *Encyclopedia of Applied and Computational Mathematics*; Engquist, B., Ed.; Springer: Berlin/Heidelberg, Germany, 2015; pp. 1–5. [CrossRef]
67. Tinsley Oden, J. A Posteriori Error Estimation, 2002. In Verification and Validation in Computational Solid Mechanics. Hans Maier (Ed.), ASME/USACM Standards (2002). Available online: https://users.oden.utexas.edu/~oden/Dr._Oden_Reprints/2001-013.a_posteriori-draft.pdf (accessed on 8 July 2023).
68. Iannizzaro, V.; Messina, B.; Cundari, M.R. Applications of integrated survey for historical heritage's knowledge: Digital modeling of the Villa Rufolo's moorish cloister in Ravello. *Int. Arch. Photogramm. Remote Sens. Spat. Inf. Sci.* **2013**, *XL-5/W2*, 361–366. [CrossRef]
69. Cignoni, P.; Callieri, M.; Corsini, M.; Dellepiane, M.; Ganovelli, F.; Ranzuglia, G. MeshLab: An open-source mesh processing tool. In Proceedings of the Sixth Eurographics Italian Chapter Conference, Salerno, Italy, 2–4 July 2008; Scarano, V., Chiara, R.D., Erra, U., Eds.; Eurographics Association: Eindhoven, The Netherlands, 2008; pp. 129–136. [CrossRef]
70. Visual Computing Lab, CNR-ISTI. MeshLab. Available online: https://www.meshlab.net/ (accessed on 15 July 2023).
71. Blender Foundation. Blender. Available online: https://www.blender.org/ (accessed on 15 July 2023).
72. French, G. gSculpt. Available online: https://gsculpt.sourceforge.net/index.html (accessed on 15 July 2023).
73. Pixologic. ZBrush. Available online: https://www.maxon.net/en/zbrush (accessed on 15 July 2023).
74. da Silva, A.P.C.M. Retopology: A Comprehensive Study of Current Automation Solutions from an Artist's Workflow Perspective. Master's Thesis, Universidade do Minho, Escola de Engenharia, Departamento de Informatica, Braga, Portugal, 2019. [CrossRef]
75. Stoker, J. *Differential Geometry*; Wiley Classics Library, Wiley: Hoboken, NJ, USA, 1989. [CrossRef]
76. Angelillo, M.; Babilio, E.; Fortunato, A. Folding of thin walled tubes as a free gradient discontinuity problem. *J. Elast.* **2006**, *82*, 243–271. [CrossRef]
77. Angelillo, M.; Babilio, E.; Fortunato, A. Singular stress fields for masonry-like vaults. *Contin. Mech. Thermodyn.* **2013**, *25*, 423–441. [CrossRef]
78. Gabellone, F. Principi e metodi dell'archeologia ricostruttiva. Dall'approccio filologico alla ricostruzione tipologica. *Archeol. Calc.* **2021**, *32*, 213–232. [CrossRef]